Biochemical and Biophysical Research Communications 448 (2014) 195–199

Contents lists available at ScienceDirect

Biochemical and Biophysical Research Communications

journal homepage: www.elsevier.com/locate/ybbrc

Simultaneous measurement of a range of particle sizes during $A\beta_{1-42}$ fibrillogenesis quantified using fluorescence correlation spectroscopy

Judith J. Mittag [a], Silvia Milani [a], Dominic M. Walsh [b], Joachim O. Rädler [a], Jennifer J. McManus [c,*]

[a] Ludwig-Maximilians-Universität, Fakultät für Physik & CeNS, Geschwister-Scholl-Platz 1, 80539 München, Germany
[b] Laboratory for Neurodegenerative Research, Center for Neurologic Diseases, Brigham & Women's Hospital, Harvard Institutes of Medicine, Boston, MA 02115, USA
[c] Department of Chemistry, National University of Ireland Maynooth, Maynooth, Co. Kildare, Ireland

ARTICLE INFO

Article history:
Received 7 April 2014
Available online 24 April 2014

Keywords:
Fluorescence correlation spectroscopy
Amyloid beta
Aggregation
Oligomerization
Alzheimer's disease
Protein folding disease

ABSTRACT

Low molecular weight oligomers of amyloid beta (Aβ) are important drivers of Alzheimer's disease. A decrease in Aβ monomer levels in human cerebrospinal fluid (CSF) is observed in Alzheimers' patients and is a robust biomarker of the disease. It has been suggested that the decrease in monomer levels in CSF is due to the formation of Aβ oligomers. A robust technique capable of identifying Aβ oligomers in CSF is therefore desirable. We have used fluorescence correlation spectroscopy and a five Gaussian distribution model (5GDM) to monitor the aggregation of $A\beta_{1-42}$ in sodium phosphate buffer and in artificial cerebrospinal fluid (ACSF). In buffer, several different sized components (monomer, oligomers, protofibrils and fibrils) can be identified simultaneously using 5GDM. In ACSF, the faster kinetics of fibrillogenesis leads to the formation of fibrils on very short timescales. This analysis method can also be used to monitor the aggregation of other proteins, nanoparticles or colloids, even in complex biological fluids.

1. Introduction

The accumulation of fibrils formed from the amyloid beta-protein (Aβ) is a defining pathological hallmark of Alzheimer's disease (AD) [1]. However, recent evidence suggests that low molecular weight (M_W) diffusible aggregates of Aβ (commonly referred to as Aβ oligomers) are more important drivers of AD than the Aβ fibrils found in amyloid deposits [2–4]. Several studies have shown that small protein aggregates are cytotoxic and contribute to synaptic dysfunction [5–10]. In nature, there are at least 20 different Aβ alloforms all of which have the same common core of about 30 residues, but differ in the length of their N- and C-termini [11]. Within this family of peptides, primary sequences terminating at Ala42 are particularly associated with AD [12].

A lowering of $A\beta_{1-42}$ monomer levels in human cerebrospinal fluid (CSF) has been widely validated as a robust biomarker for the diagnosis of AD [13], including in pre-symptomatic individuals that subsequently developed AD [14,15]. Mechanistically, the progressive accumulation of both soluble and insoluble Aβ aggregates has been postulated to explain the decline in $A\beta_{1-42}$ monomer observed in CSF. Consequently, it is believed that measurement of Aβ oligomer levels in CSF could offer an even more sensitive indicator than current biomarkers [13]. Despite intense efforts there are currently no validated, reliable and sensitive means to detect Aβ oligomers in CSF. The oligomerization and subsequent formation of protein fibrils of Aβ is a complex interplay of many peptides and mechanisms and is not yet fully understood [16–20]. However, the majority of studies find that the mechanism for fibrillogenesis is consistent with a nucleation-dependent polymerization model [5,18,21] as illustrated in Fig. 1(A). More recent work has suggested that a second nucleation step occurs [22].

The major difficulty in monitoring the progression of Aβ fibrillogenesis is the range of particles sizes present. Even at the early stages of fibrillogenesis Aβ will exist as monomer, heterogenous oligomers, protofibrils and fibrils. Few techniques can measure and track the components of such a heterogenous mixture of different sized species simultaneously. Several methods have been used to map the progression of peptide aggregation, from monomer to fibril, including, high performance liquid chromatography, gel electrophoresis, atomic force microscopy, transmission electron microscopy (TEM), Thioflavin T assays, dynamic light scattering and others [16]. Monomeric Aβ has a hydrodynamic radius (R_h)

Abbreviations: Aβ, amyloid β-protein; $A\beta_{1-42}$, Aβ spanning residues from Asp1 to Ala42; AD, Alzheimer's disease; CSF, cerebrospinal fluid; 5GDM, five Gaussian distribution model; FCS, fluorescence correlation spectroscopy; MEMFCS, maximum entropy method for FCS data analysis; M_W, molecular weight.

* Corresponding author.
E-mail addresses: judith.mittag@physik.lmu.de (J.J. Mittag), silvia.milani@physik.lmu.de (S. Milani), dwalsh3@partners.org (D.M. Walsh), raedler@lmu.de (J.O. Rädler), Jennifer.mcmanus@nuim.ie (J.J. McManus).

http://dx.doi.org/10.1016/j.bbrc.2014.04.088
0006-291X/

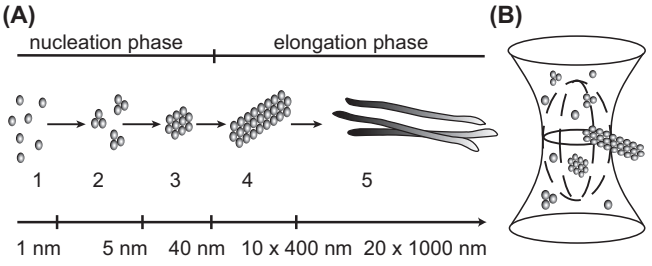

Fig. 1. (A) The standard nucleation-dependent polymerization (single nucleation) model for amyloid aggregation: formation of fibrils proceeds through a multistage process. Monomers (1) form low molecular weight aggregates (2), then higher molecular weight aggregates (3) in the nucleation stage, which has a characteristic lag time before the formation of protofibrils (4) and fibrils (5). A secondary nucleation step leading to the formation of oligomers via a fibril-catalyzed process has also been suggested [22] (not shown). (B) The confocal volume for FCS measurements: fluorescently labeled monomers and peptides diffuse into and out of the confocal volume leading to fluctuations in the fluorescence signal.

of 0.9 ± 0.1 nm [23], while oligomeric and fibril forms range in size from several nanometers to several microns [16–19].

It is challenging to quantitatively measure the sizes of different oligomers, which co-exist with Aβ monomer, protofibrils and fibrils during a typical measurement. Fluorescence correlation spectroscopy (FCS) can be used to differentiate multiple components in a polydisperse solution and has already been used to study the aggregation of other amyloidogenic proteins. Notably, the aggregation of polyglutamine in cells [24], α-synuclein aggregation [25] and its binding to vesicles [26] have been studied. In relation to Aβ, FCS has been used to establish an in vitro saturation concentration of $A\beta_{1-40}$ [27], to test the interaction with aggregation inhibitors [28] and membranes [29,30], to study the depletion of oligomers under physiological conditions [23] and to determine the size distribution of $A\beta_{1-40}$ aggregates in solution [27,31,32]. Garai et al. [27] used a maximum entropy fitting method (MEMFCS), which allowed multiple aggregating species within the system to be analyzed. While this is an improvement over standard fitting methods, it did not distinguish clearly between the oligomeric species in solution. Therefore, a need for a fitting procedure which can distinguish more clearly the different sized forms of Aβ during fibrillogenesis exists.

Here, we have approached this problem by defining several sizes ranges (up to five) as Gaussian profiles (5GDM) and using these to fit the FCS autocorrelation function. This allows each pre-defined component to be fit to the data simultaneously, allowing more of the different sized components in the aggregating system to be determined at any particular time point during the experiment. The size distributions obtained using 5GDM analysis are compared to those obtained using MEMFCS. To our knowledge no previous work has used such a high number of Gaussian-shaped peaks and the same free variables for analysis of FCS data for polydisperse systems. This approach is not specific to Aβ, and we expect that it will be readily applied to study of other aggregating or amyloidogenic proteins.

2. Material and methods

2.1. Sample preparation

Synthetic $A\beta_{1-42}$ was purchased from W. M. Keck Biotechnology Facility at Yale University and Hilyte Fluor488™ labeled $A\beta_{1-42}$ was purchased from Anaspec Inc., Fremont (CA). The latter was dissolved in 1% NH_4OH and diluted to a final concentration of 1 mg/ml in 10 mM sodium phosphate buffer [33]. $A\beta_{1-42}$ was dissolved in 0.1% NH_4OH and then diluted with 100 mM Tris buffer at 1 mM, aliquoted and stored at −20 °C. Once thawed, peptide solutions were centrifuged at 100,000*g* and 4 °C for 1 h in a Beckman Optima Max XP ultracentrifuge (Indianapolis, IN) to remove pre-existing fibrils. The upper 75% of the supernatant was collected and the concentration of $A\beta_{1-42}$ determined by absorbance at 275 nm. Thereafter the supernatant was further diluted to the desired concentrations using 10 mM sodium phosphate buffer or artificial CSF (119 mM NaCl, 26.2 mM $NaHCO_3$, 2.5 mM KCl, 1 mM NaH_2PO_4, 1.3 mM $MgSO_4$-$7H_2O$, 11 mM D-(+)-Glucose and 2.5 mM $CaCl_2.2H_2O$, pH adjusted to 7.3–7.4).

2.2. FCS experiments

FCS measurements were performed on a LSM10 microscope equipped with a ConfoCor2 unit (Carl Zeiss Jena, Germany), a 488 nm Argon laser and an apochromatic 40× water-immersion objective with a NA of 1.2. Fluorescence emission was separated from laser light using a bandpass filter (505–550 nm). Calibration was performed with Alexa 488 to determine the dimensions of the observation volume. Samples were filled in NUNC 8-Well-Plates (Thermo Scientific), which were coated with 15 μg/ml poly-L-lysine (Biochrom AG). All measurements were performed at room temperature. Autocorrelation functions obtained from FCS measurements were analyzed as described in Supplementary information.

3. Results and discussion

3.1. Aggregation of $A\beta_{1-42}$ in sodium phosphate buffer

The aggregation of $A\beta_{1-42}$ was measured at 10 and 20 μM in the presence of 0.01% labeled $A\beta_{1-42}$ in 10 mM sodium phosphate buffer, pH 7.4 by FCS. Variability in the time before onset of oligomer formation can depend on preparation conditions [16], and/or additional stresses applied to the sample to speed up the process [25,34–36]. Measurements were taken systematically over 48 h using consistent preparation methods to minimize these effects. Fig. 2 shows the evolution of an autocorrelation function over the time course of a typical experiment. This sample, at 20 μM, indicates that higher M_W species appear over several hours, indicated by a shift in the delay time to higher values.

3.2. Comparison of MEMFCS and 5GDM fitting

Beyond the first few measurements, a one-component fit (SI Eq. (2)) leads to unsatisfactory and physically unrealistic results (not shown). Thus, a more sophisticated fitting method is required.

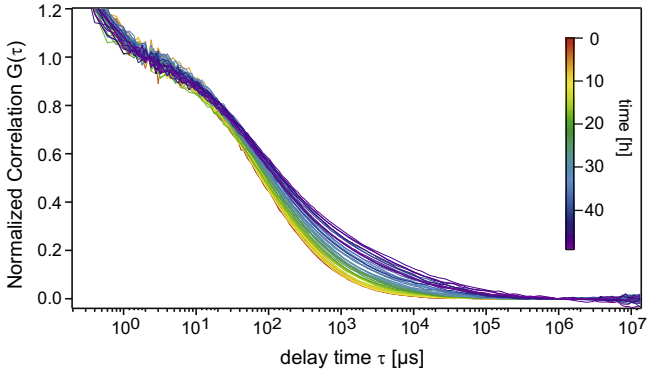

Fig. 2. Normalized average correlation curves over 48 h for a 20 μM $A\beta_{1-42}$ sample (0.01% labeled). During the experiment the curves shift to the right and a buckling develops, indicating an increase in the number of different species and of particle sizes.

We first applied the MEMFCS fitting method [27,37] to autocorrelation functions at different time points throughout the experiment (Fig. 3A). A fit of the first measurement, reveals a single peak with a R_h maximum at 1.44 nm and a shoulder towards larger hydrodynamic radii. After 48 h, three peaks corresponding to spherical hydrodynamic radii of 2.09 nm, 101.17 nm and 4.5 μm were observed (Fig. 3E).

Due to the assumption of maximum uncertainty and to avoid over interpretation of the data, MEMFCS fitting finds the widest size distribution that is consistent with the data [37]. Thus, the broad peaks obtained with MEMFCS are likely to include size distribution data for several different species in solution. Distribution curves resulting from MEMFCS analysis show Gaussian-type distribution features. Therefore, we used a Gaussian-shaped size distribution with a fixed number of peaks to fit our experimental data. This was inspired by initial work by Pal et al. [38], who used this approach as an alternative to MEMFCS for microemulsion droplets. The idea is that a component is not monodisperse with a single value for the diffusion time, τ_D, but rather a Gaussian distribution on a logarithmic time-scale with a peak diffusion time τ_P. The fit to the autocorrelation function is described by:

$$G(\tau) = \sum_{i=1}^{n} a_i(\tau_{Di}) \left(\frac{1}{1+\frac{\tau}{\tau_{Di}}}\right)\left(\frac{1}{1+\frac{\tau}{\omega^2\tau_{Di}}}\right)^{\frac{1}{2}} \quad (1)$$

with the amplitude distribution

$$a_i(\tau_{Di}) = \sum_{n=1}^{k} A_n \exp\left[-\left(\frac{\ln(\tau_{Di}) - \ln(\tau_{Pn})}{b_n}\right)\right] \quad (2)$$

where A_n is the relative amplitude of the components, τ_{Pn} is the peak diffusion time of the nth component and b_n is related to the width of the distribution. The τ_D's have the same logarithmic quasi-continuous distribution as for MEMFCS. We have extended the work of Pal et al. by varying A_n, τ_{Pn} and b_n rather than using only a single peak. The fraction of each of the components was then determined by calculating the areas under the Gaussian peaks and normalizing them by the sum of the peak areas:

$$\text{Fraction}_n = \frac{\text{area}_n}{\sum_{n=1}^{k}\text{area}_n} \quad (3)$$

Hence, each distribution in the Gaussian distribution model (GDM) will represent a narrow range of particle sizes. The validity of the GDM was verified by extensive testing of the well-known dye Alexa 488 (using one distribution successfully, whereas a higher number of distributions were rejected by the model correctly). We choose to use five peaks for the fitting of Aβ since this was a good balance between distinguishing the different species in solution (monomer, small oligomer, larger oligomer, protofibril and fibril) and not having so many free variables that the outcome of the fits was physically unrealistic. Analysis of many autocorrelation curves using this method, gave consistent results. Less than five peaks led to an inappropriate description of the system (i.e. component sizes smaller than monomeric Aβ concomitant with very large particles at early time points).

In Fig. 3B the results of the analysis with the 5GDM are presented. There are a larger number of more sharply defined peaks representing different levels of $A\beta_{1-42}$ aggregation than for MEMFCS. 5GDM fits reveal that two peaks at 1.17 nm and 1.62 nm are present at early time points in the experiment. If a weighted sum of these first two peaks is calculated using the relative amplitudes, a R_h of 1.44 nm is determined. This corresponds exactly to the diffusion time for the first peak obtained using MEMFCS fitting. In Fig. 3C–E, a direct comparison of the results of both fitting methods is shown for measurements taken at 0 h, 20 h and 48 h. For all three time points the results of 5GDM and MEMFCS are in good agreement and show the same trends for the aggregating system. However, at the later time points (48 h) significant differences for the calculated size of fibrils are observed (R_h = 4.5 μm for MEMFCS and R_h = 0.85 μm for 5GDM). These particle sizes are beyond

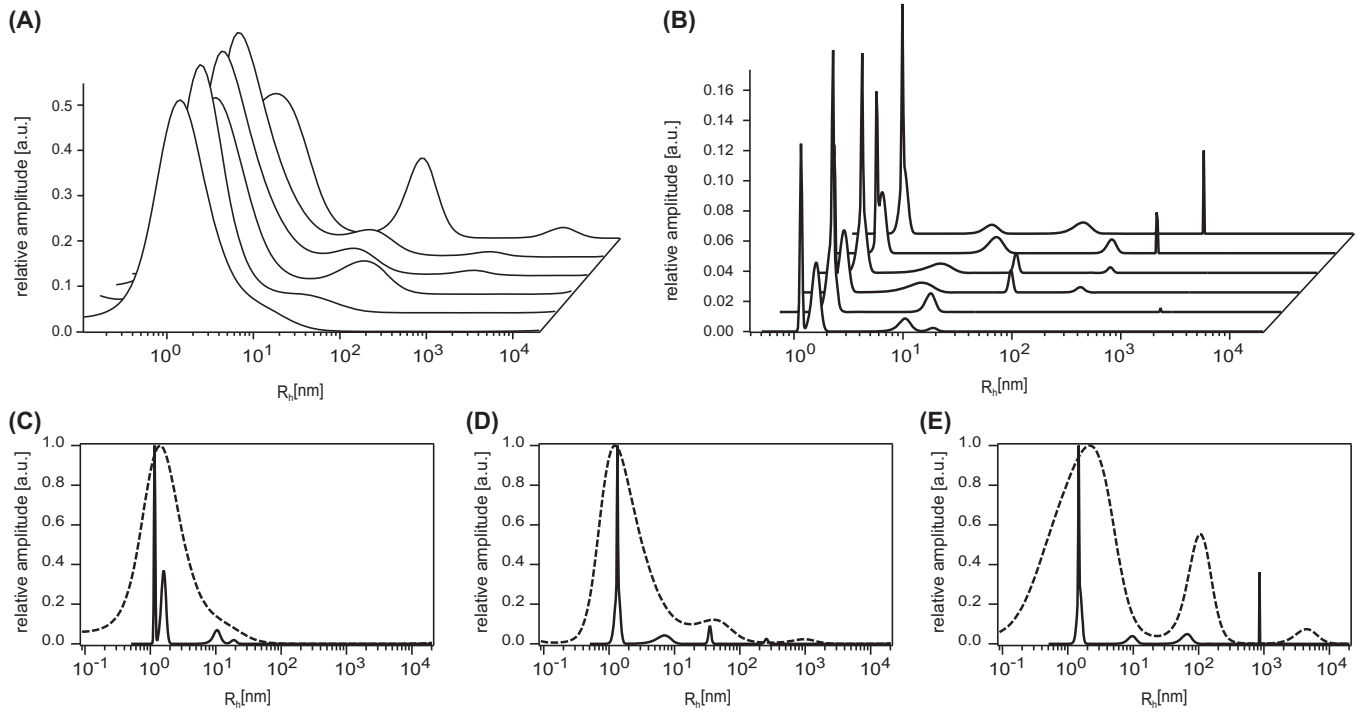

Fig. 3. Size distribution obtained with (A) MEMFCS and (B) 5GDM. Both fitting methods show similar trends, but the GDM fitting provides sharper and more defined peaks, especially in the range of low M_W oligomers. Measurements at 0 h, 5 h, 16 h, 20 h, 40 h and 48 h. (C–E) direct comparison of the results of MEMFCS (dashed) and 5GDM (line) for (C) 0 h, (D) 20 h and (E) 48 h. Both fitting methods show the same trends.

the reasonable measureable range for FCS and the values are artifacts of the fitting procedure in both methods. A comparison of the results obtained for each fitting procedure is shown in Fig. 3C–E. Clearly the general features of the aggregating system are consistent using both methods, but the 5GDM provides a more detailed and potentially a more realistic description of the aggregating system with better resolution of low M_W species.

3.3. Evaluation of the four fractions of $A\beta_{1-42}$ aggregates

5GDM reveals a larger number of species within the system than MEMFCS, but each of these species represents a range of particle sizes. Since the first two peaks fuse and separate several times during the experiment, it was impossible to analyze these fractions separately (Fig. 3D and E). Hence, the percentages of the first two peaks were pooled and treated as one. This leads to a four level fraction model for $A\beta_{1-42}$ aggregation (although a five peak fitting formula is used). The fusion of these first two peaks is probably due to a dynamic equilibrium that is assumed between monomers and very small oligomers [39,40]. We have therefore defined each of the size ranges obtained from the fitting as: (1) small components including monomers and low M_W oligomers; (2) higher M_W oligomers; (3) protofibrils and (4) fibrils. The fractions of the various Aβ particles in solution were determined from the 5GDM fitting and calculated using Eq. (3). The fractions were monitored over time and the averaged values are shown in Fig. 4.

The rate of aggregation is slower in the lower concentration samples and is consistent with previous experiments [32]. After 48 h, the proportion of fraction 1 (monomer and small oligomers) is higher in the lower concentration samples (72.4 for 10 μM compared to 64.9% for 20 μM), with a corresponding lower proportion of fibrils (3.6% for 10 μM and 7.5% for 20 μM). The proportion of fraction 1 decreases as fibrillogenesis proceeds (Fig. 4), while the R_h stays relatively constant (Fig. S1). Combined, these observations indicate a real decrease of the amount of monomer/small oligomers in solution. In Fig. S1 the evolution of the two peaks, which we have called fraction 1 (monomer and small oligomer) is shown. We observe that only a few data points lie in the monomer range between 0.8 and 1 nm [23], and most of the data points lie between 1 and 2 nm. This size range represents mixtures of monomers and small oligomers. Therefore with 5GDM it is not possible to differentiate between monomers and small oligomers and hence we have pooled this data in fraction 1. However, we can clearly separate a mixture of monomers and low M_W oligomers from larger aggregates. At the beginning of an experiment the dominating species are small components (Fig. 4). This starting material consists of a mixture of monomer and small oligomers. Monomeric samples did not aggregate on a reasonable experimental time scale [23]. Examining fraction 2 (higher Mw oligomers), we see that these remain constant throughout the experiment (Fig. 4) (14% for 10 μM and 19% for 20 μM). For this fraction, the R_h grows slowly in size, and is in the range of 10 nm (Fig. S2). Hence, before the first measurement, equilibrium between small components (fraction 1) and high M_W oligomers (fraction 2) is established.

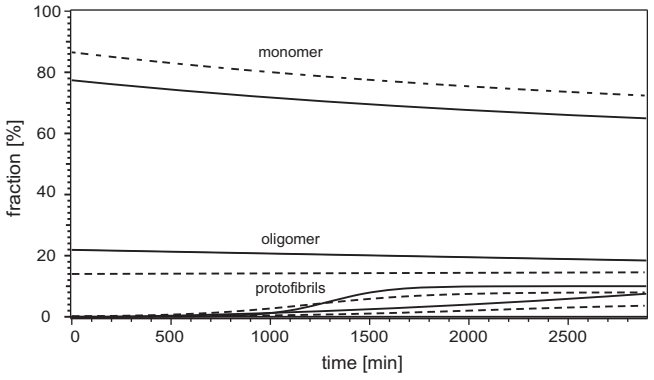

Fig. 4. Development of the fractions of the four aggregate levels of $A\beta_{1-42}$ in sodium phosphate buffer, dashed lines represent 10 μM Aβ samples, solid lines represent 20 μM measurements. The amount of small components/monomers decreases over time, while the amount of protofibrils and fibrils increases after a certain lag time. The fraction of high M_W oligomers stays constant. The experiments were preformed in triplicate to ensure reproducibility.

Protofibrils or fibrils are not present in FCS data at the beginning of the experiment (Fig. 4), but appear after a lag time, consistent with a nucleation-dependent polymerization model [41]. Both species show a sigmoidal behavior and a mean lag time of ~16 h. The fraction of protofibrils reaches a saturation level of 10% at 20 μM and 8% at 10 μM, respectively, while the proportion of fibrillar material continues to increase to the end of the experiment. Transmission electron microscopy (TEM) confirmed fibril formation (Fig. S3). The presence of fibrils is consistent with 5GDM analysis and the size values obtained for fibrils are in agreement with published studies [5,42,43].

3.4. Preliminary experiments in artificial CSF

Using artificial cerebrospinal fluid (ACSF), we assessed if the 5GDM fitting procedure is suitable for analysis in complex buffers and potentially in biological fluids. Large sedimenting particles are observed immediately after mixing stock Aβ with ACSF. During FCS measurements, this manifests as decreasing particle numbers due to loss of material to the large aggregates. The remaining monomeric material, now at much lower concentration, does not proceed to form higher M_W oligomers, since it is below the concentration required for the onset of fibrillogenesis. The higher ionic strength of ACSF leads to much faster kinetics for fibrillogenesis of $A\beta_{1-42}$ in μM concentrations [36]. An incremental decrease in Aβ, to nM concentrations, failed to find a regime in which a broader distribution of particles sizes was observed. Furthermore, adding labeled Aβ to pre-aggregated samples in ACSF produced similar results. In these experiments, only single events in the count rate plots were observed for 1 μM, 500 nM and 50 nM $A\beta_{1-42}$, and these bursts corresponded to fibrils rather than to oligomers. A systematic evaluation with 5GDM was not performed, since these single events do not meet the requirements of the statistical basis needed for quantitative FCS analysis. These observations are consistent with Nag et al. [23]. They suggested that $A\beta_{1-42}$ aggregation is dependent on physiological factors at low concentrations of $A\beta_{1-42}$ and that aggregates dissociate below a certain concentration because they are thermodynamically unstable. However, beyond the limitation of this experimental system, there are no technical barriers to using 5GDM analysis in ACSF, CSF or other complex biological fluids.

A new fitting procedure for FCS (5GDM), allowing several different sized components in solution to be analyzed simultaneously has been developed to study the fibrillogenesis of $A\beta_{1-42}$. Four $A\beta_{1-42}$ aggregate types in solution were identified; small components (including monomer and low molecular weight oligomers), high M_W oligomers, protofibrils and fibrils. Each component was observed in solution over 48 h for a range of protein concentrations. A comparison with MEMFCS analysis confirmed that the results obtained with 5GDM are consistent with the established method, but that better resolution of particle size distributions in the nm range were obtained using 5GDM. Given that oligomers of Aβ in CSF have been found at picogram levels [44], concentration of the sample to pM levels could facilitate measurements in CSF using FCS with 5GDM. This analysis method could also be usefully employed to monitor the aggregation of other proteins, nanoparticles and colloids.

Acknowledgments

This work was made possible by funding from Science Foundation Ireland Stokes Lectureship (to J.J.McM), European Science Foundation networking programme "epitopeMap" (grant to J.O.R and J. J. McM), EU FP7 (NanoTransKinetics grant to JM, JOR), Deutsche Forschungsgemeinschaft (JM, travel grant) and the Foundation for Neurologic Diseases (DMW).

Appendix A. Supplementary data

Supplementary data associated with this article can be found, in the online version, at http://dx.doi.org/10.1016/j.bbrc.2014.04.088.

References

[1] C.L. Masters, G. Simms, N.A. Weinman, et al., Amyloid plaque core protein in Alzheimer disease and Down syndrome, Proc. Natl. Acad. Sci. U.S.A. 82 (1985) 4245–4249.
[2] L.N. Zhao, H. Long, Y. Mu, et al., The toxicity of amyloid beta oligomers, Int. J. Mol. Sci. 13 (2012) 7303–7327.
[3] D.M. Walsh, D.J. Selkoe, A beta oligomers – a decade of discovery, J. Neurochem. 101 (2007) 1172–1184.
[4] I. Benilova, E. Karran, B. De Strooper, The toxic Abeta oligomer and Alzheimer's disease: an emperor in need of clothes, Nat. Neurosci. 15 (2012) 349–357.
[5] D.M. Walsh, D.M. Hartley, Y. Kusumoto, et al., Amyloid beta-protein fibrillogenesis. Structure and biological activity of protofibrillar intermediates, J. Biol. Chem. 274 (1999) 25945–25952.
[6] M. Hoshi, M. Sato, S. Matsumoto, et al., Spherical aggregates of beta-amyloid (amylospheroid) show high neurotoxicity and activate tau protein kinase I/glycogen synthase kinase-3beta, Proc. Natl. Acad. Sci. U.S.A. 100 (2003) 6370–6375.
[7] S. Barghorn, V. Nimmrich, A. Striebinger, et al., Globular amyloid beta-peptide oligomer – a homogenous and stable neuropathological protein in Alzheimer's disease, J. Neurochem. 95 (2005) 834–847.
[8] S. Lesne, M.T. Koh, L. Kotilinek, et al., A specific amyloid-beta protein assembly in the brain impairs memory, Nature 440 (2006) 352–357.
[9] G.M. Shankar, S. Li, T.H. Mehta, et al., Amyloid-beta protein dimers isolated directly from Alzheimer's brains impair synaptic plasticity and memory, Nat. Med. 14 (2008) 837–842.
[10] M. Lambert, A. Barlow, Diffusible, nonfibrillar ligands derived from $A\beta_{1-42}$ are potent central nervous system neurotoxins, Proc. Natl. Acad. Sci. U.S.A. 95 (1998) 6448–6453.
[11] E. Portelius, A. Westman-Brinkmalm, H. Zetterberg, et al., Determination of beta-amyloid peptide signatures in cerebrospinal fluid using immunoprecipitation-mass spectrometry, J. Proteome Res. 5 (2006) 1010–1016.
[12] B. De Strooper, Proteases and proteolysis in Alzheimer disease: a multifactorial view on the disease process, Physiol. Rev. 90 (2010) 465–494.
[13] D.M. Holtzman, CSF biomarkers for Alzheimer's disease: current utility and potential future use, Neurobiol. Aging 32 (Suppl 1) (2011) S4–S9.
[14] R.J. Bateman, C. Xiong, T.L. Benzinger, et al., Dominantly inherited Alzheimer, clinical and biomarker changes in dominantly inherited Alzheimer's disease, N. Engl. J. Med. 367 (2012) 795–804.
[15] L.M. Peder Buchhave, K.B. Henrik Zetterberg, Asa K. Wallin, et al., Cerebrospinal fluid levels of beta-amyloid 1–42, but not of tau, are fully changed already 5–10 years before the onset of Alzheimer dementia, Arch. Gen. Psychiatry 69 (2012) 98–106.
[16] N.E. Pryor, M.A. Moss, C.N. Hestekin, Unraveling the early events of amyloid-beta protein (Abeta) aggregation: techniques for the determination of Abeta aggregate size, Int. J. Mol. Sci. 13 (2012) 3038–3072.
[17] J.M. Paredes, S. Casares, M.J. Ruedas-Rama, et al., Early amyloidogenic oligomerization studied through fluorescence lifetime correlation spectroscopy, Int. J. Mol. Sci. 13 (2012) 9400–9418.
[18] S. Kumar, N. Rezaei-Ghaleh, D. Terwel, et al., Extracellular phosphorylation of the amyloid beta-peptide promotes formation of toxic aggregates during the pathogenesis of Alzheimer's disease, EMBO J. 30 (2011) 2255–2265.
[19] L.A. Munishkina, A.L. Fink, Fluorescence as a method to reveal structures and membrane-interactions of amyloidogenic proteins, Biochim. Biophys. Acta 1768 (2007) 1862–1885.
[20] Y. Liang, D.G. Lynn, K.M. Berland, Direct observation of nucleation and growth in amyloid self-assembly, J. Am. Chem. Soc. 132 (2010) 6306–6308.
[21] E. Hellstrand, B. Boland, D.M. Walsh, et al., Amyloid beta-protein aggregation produces highly reproducible kinetic data and occurs by a two-phase process, ACS Chem. Neurosci. 1 (2010) 13–18.
[22] S.I. Cohen, S. Linse, L.M. Luheshi, et al., Proliferation of amyloid-beta42 aggregates occurs through a secondary nucleation mechanism, Proc. Natl. Acad. Sci. U.S.A. 110 (2013) 9758–9763.
[23] S. Nag, B. Sarkar, A. Bandyopadhyay, et al., Nature of the amyloid-beta monomer and the monomer–oligomer equilibrium, J. Biol. Chem. 286 (2011) 13827–13833.
[24] Y. Takahashi, Y. Okamoto, H.A. Popiel, et al., Detection of polyglutamine protein oligomers in cells by fluorescence correlation spectroscopy, J. Biol. Chem. 282 (2007) 24039–24048.
[25] S. Nath, J. Meuvis, J. Hendrix, et al., Early aggregation steps in alpha-synuclein as measured by FCS and FRET: evidence for a contagious conformational change, Biophys. J. 98 (2010) 1302–1311.
[26] E. Rhoades, T.F. Ramlall, W.W. Webb, et al., Quantification of alpha-synuclein binding to lipid vesicles using fluorescence correlation spectroscopy, Biophys. J. 90 (2006) 4692–4700.
[27] K. Garai, B. Sahoo, P. Sengupta, et al., Quasihomogeneous nucleation of amyloid beta yields numerical bounds for the critical radius, the surface tension, and the free energy barrier for nucleus formation, J. Chem. Phys. 128 (2008) 045102.
[28] K. Wiesehan, J. Stohr, L. Nagel-Steger, et al., Inhibition of cytotoxicity and amyloid fibril formation by a D-amino acid peptide that specifically binds to Alzheimer's disease amyloid peptide, Protein Eng. Des. Sel. 21 (2008) 241–246.
[29] S. Hossain, M. Grande, G. Ahmadkhanov, et al., Binding of the Alzheimer amyloid beta-peptide to neuronal cell membranes by fluorescence correlation spectroscopy, Exp. Mol. Pathol. 82 (2007) 169–174.
[30] B. Sarkar, A.K. Das, S. Maiti, Thermodynamically stable amyloid-beta monomers have much lower membrane affinity than the small oligomers, Front. Physiol. 4 (2013) 84.
[31] L.O. Tjernberg, A. Pramanik, S. Bjorling, et al., Amyloid beta-peptide polymerization studied using fluorescence correlation spectroscopy, Chem. Biol. 6 (1999) 53–62.
[32] P. Sengupta, K. Garai, B. Sahoo, et al., The amyloid beta peptide (A beta(1–40)) is thermodynamically soluble at physiological concentrations, Biochemistry-US 42 (2003) 10506–10513.
[33] β-Amyloid (1–42), HiLyte Fluor™ 488-labeled Product Data Sheet, Anaspec Inc.
[34] P. Cizas, R. Budvytyte, R. Morkuniene, et al., Size-dependent neurotoxicity of beta-amyloid oligomers, Arch. Biochem. Biophys. 496 (2010) 84–92.
[35] C. Cabaleiro-Lago, F. Quinlan-Pluck, I. Lynch, et al., Dual effect of amino modified polystyrene nanoparticles on amyloid beta protein fibrillation, ACS Chem. Neurosci. 1 (2010) 279–287.
[36] V.H. Finder, R. Glockshuber, Amyloid-beta aggregation, Neurodegener. Dis. 4 (2007) 13–27.
[37] P. Sengupta, K. Garai, J. Balaji, et al., Measuring size distribution in highly heterogeneous systems with fluorescence correlation spectroscopy, Biophys. J. 84 (2003) 1977–1984.
[38] N. Pal, S. Dev Verma, M.K. Singh, et al., Fluorescence correlation spectroscopy: an efficient tool for measuring size, size-distribution and polydispersity of microemulsion droplets in solution, Anal. Chem. 83 (2011) 7736–7744.
[39] A. Jan, D.M. Hartley, H.A. Lashuel, Preparation and characterization of toxic Abeta aggregates for structural and functional studies in Alzheimer's disease research, Nat. Protoc. 5 (2010) 1186–1209.
[40] S.A. Funke, Detection of soluble amyloid-beta oligomers and insoluble high-molecular-weight particles in CSF: development of methods with potential for diagnosis and therapy monitoring of Alzheimer's disease, Int. J. Alzheimers Dis. 2011 (2011) 151645.
[41] S. Kumar, J. Walter, Phosphorylation of amyloid beta (Aâ) peptides – a trigger for formation of toxic aggregates in Alzheimer's disease, Aging (N.Y.) 3 (2011) 1–10.
[42] C. Sachse, Elektronenmikroskopie an Alzheimer-Fibrillen, Bioforum 32 (2009) 26–28.
[43] M. Fandrich, Oligomeric intermediates in amyloid formation: structure determination and mechanisms of toxicity, J. Mol. Biol. 421 (2012) 427–440.
[44] N. Salvadores, M. Shahnawaz, E. Scarpini, et al., Detection of misfolded Abeta oligomers for sensitive biochemical diagnosis of Alzheimer's disease, Cell Rep. (2014) 1–8.